Institute of Physics Publishing Nanotechnology
Nanotechnology **17** (2006) 2294–2303 doi:10.1088/0957-4484/17/9/038

# Effects of a carbon nanotube layer on electrical contact resistance between copper substrates

**Myounggu Park[1], Baratunde A Cola[2], Thomas Siegmund[2], Jun Xu[2], Matthew R Maschmann[2], Timothy S Fisher[2] and Hyonny Kim[1,3]**

[1] School of Aeronautics and Astronautics and Birck Nanotechnology Centre, Purdue University, West Lafayette, IN 47907, USA
[2] School of Mechanical Engineering and Birck Nanotechnology Centre, Purdue University, West Lafayette, IN 47907, USA

E-mail: hyonny@purdue.edu

Received 3 January 2006
Published 7 April 2006
Online at stacks.iop.org/Nano/17/2294

**Abstract**
Reduction of contact resistance is demonstrated at Cu–Cu interfaces using a multiwalled carbon nanotube (MWCNT) layer as an electrically conductive interfacial material. The MWCNTs are grown on a copper substrate using plasma enhanced chemical vapour deposition (PECVD) with nickel as the catalyst material, and methane and hydrogen as feed gases. The MWCNTs showed random growth directions and had a bamboo-like structure. Contact resistance and reaction force were measured for a bare Cu–Cu interface and a Cu–MWCNT–Cu interface as a function of probe position. For an apparent contact area of 0.31 mm$^2$, an 80% reduction in contact resistance was observed when the MWCNT layer was used. Resistance decreased with increasing contact force, thereby making it possible to use this arrangement as a small-scale force sensor. Also, the Cu–MWCNT–Cu interface was roughly two times stiffer than the bare Cu–Cu interface. Contact area enlargement and van der Waals interactions are identified as important contributors to the contact resistance reduction and stiffness increase. A model based on compaction of the MWCNT layer is presented and found to be capable of predicting resistance change over the range of measured force.

(Some figures in this article are in colour only in the electronic version)

## 1. Introduction

Electrical contacts are vital elements in many engineering systems and applications at the macro, micro, and nano scales. Reliability and functionality of electrical contacts can often be a limiting design factor. A major portion of electrical contact resistance comes from the lack of ideal mating between surfaces. Primary causes of this problem involve the surface roughness and mechanical properties of the surfaces. When two surfaces are brought together, the actual contact area may be much smaller than the apparent contact area [1]. The contact between two surfaces can actually be thought of as the contact of several discrete points in parallel, referred to as solid spots or $\alpha$-spots [1, 2]. Thus, only the $\alpha$-spots act as conductive areas and can be a small percentage of the total area.

Since their discovery [3], carbon nanotubes (CNTs) have been studied intensively throughout many communities in science and engineering. Several researchers have reported on the mechanical, electrical, and thermal properties of individual single-wall carbon nanotubes (SWNTs) [4–8]. The electrical properties of SWNTs are affected by the chirality of the SWNTs to the degree that the SWNTs can exhibit metallic

[3] Author to whom any correspondence should be addressed.

© 2006 IOP Publishing Ltd Printed in the UK

or semiconducting electrical conductivity. The electrical transport properties of a single SWNT are well studied [9]. It has been shown that for ballistic transport and perfect contacts, a SWNT has a theoretical resistance of 6.45 kΩ, which is half of the quantum resistance $h/2e^2$ [10]. In MWCNTs, each layer within the MWCNT can have either a metallic or semiconducting band structure depending on its diameter and chirality. Owing to this variation among layers, the net electrical behaviour of a MWCNT is typically metallic and a wide range of resistance values, e.g., from 478 Ω to 29 kΩ [11], have been reported.

The use of an individual MWCNT may not be low enough to reduce contact resistance at an interface significantly. However, by using an array of MWCNTs as an interfacial layer, it is expected that numerous individual contact spots and contact area enlargement can create current flow paths through each contact, thus reducing overall resistance. An additional advantage to using CNTs is that they can tolerate high current densities [10]. Therefore, a MWCNT layer can be a potential solution to the reliability and functionality issues faced at electrical interfaces.

Previous researchers have reported on MWCNT arrays used to improve thermal and electrical interface transport properties [12, 13]. The study of Tong *et al* [13] used a vertically aligned CNT film on a silicon wafer substrate. The minimum resistance measured varied from roughly 1 to 20 Ω for different samples. However, Tong *et al* [13] did not specifically address possible contact resistance reduction mechanisms. In this study, reduction of contact resistance using a non-directionally grown MWCNT layer as an interfacial material at a Cu–Cu interface is reported, and related mechanisms such as contact area enlargement and van der Waals interactions are discussed. A model is also presented predicting the experimentally observed reduction in electrical resistance for increasing applied contact force.

## 2. Experimentation

### 2.1. Fabrication of specimen

A mechanically surface-ground (46 grit wheel) copper plate was cut into 10 mm × 10 mm × 0.5 mm blocks using a water jet cutter. The copper blocks were cleaned using toluene, acetone, and methanol in an ultrasonic tank. Copper (Alloy 110; Electrolytic Tough Pitch Copper) was chosen as the substrate material due to its low electrical resistivity of $1.72 \times 10^{-8}$ Ω m, an attribute that is desired for accurately measuring the electrical resistance of Cu–Cu contacts with a MWCNT layer. Note that pure copper is used widely in the electrical industry due to its excellent electrical conductivity, bettered only by silver ($1.47 \times 10^{-8}$ Ω m) among industrial pure metals [14].

Three metal layers of Ti, Al, and Ni (thickness: 30, 10, and 6 nm respectively) were deposited on one side of the copper substrate using electron-beam evaporation. The Ti layer promotes adhesion of MWCNT to the copper substrate. The Al layer acts as a 'buffer' layer which is known to enhance the CNT growth with the Ni catalyst [12, 15, 16] that provides seed sites for CNT growth [17, 18]. The CNTs were grown on this substrate surface by a microwave plasma enhanced chemical vapour deposition (PECVD) process [12]. The feed gases were $H_2$ and $CH_4$. The flow rates of $H_2$ and $CH_4$ were 72 and 8 sccm respectively. The $H_2$ plasma was maintained under a microwave power of 150 W. The process temperature was 800 °C, and the growth time was 20 min. An as-fabricated MWCNT layer on Cu substrate is shown in figure 1. The black surface visible in the photo is the MWCNT layer.

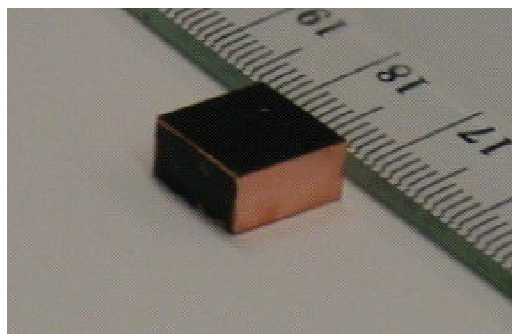


**Figure 1.** As-fabricated MWCNT layer on Cu substrate (unit = cm).

### 2.2. Characterization of specimen

The sample surface was observed using field emission scanning electron microscopy (FE-SEM). The grooves visible on the sample surface in figure 2(a) are machining lines caused by mechanical surface finishing of the copper. The magnified view of a machining groove is shown in figure 2(b). MWCNTs are observed to grow on both the 'hill' and in 'valley' regions of the machining grooves. The overall CNT layer does not show any preferred direction (see figure 2(c)). The individual CNTs have a bamboo-like structure, which is a typical feature of relatively large diameter MWCNTs (figure 2(d)).

The surface height profile and roughness of the MWCNT layer was obtained using a Veeco DI 3100 atomic force microscope (AFM). The AFM was operated under contact mode with a contact force ranging from $10^{-8}$ to $10^{-6}$ N in an ambient atmosphere [19]. In figure 3(a), the 3D surface height profile is shown, and very small peaks are observed. The mean roughness value of the MWCNT layer at a peak location (square region in figure 3(b)) is 122 nm. For comparison, the surface roughness of a silicon on insulation (SOI) wafer is 1–2 nm [20] and for a polished metal surface the roughness is 800 nm. Thus, the MWCNT layer is relatively rough compared with a SOI wafer but smoother than mechanically polished metal. The height profile of the MWCNT layer (figure 3(a)) indicates that the surface also has some sharp peak features.

### 2.3. Test setup

A schematic of the test setup is shown in figure 4. While subjecting the MWCNT-enhanced Cu substrate to compressive loading using a Cu probe, electrical resistance change was monitored by a multimeter (Hewlett Packard 3478A). To precisely measure small resistance changes, a four wire (point) measurement scheme was adopted. This method eliminates wire connection resistance, and thereby permits pure contact resistance measurement at the interface. The probe material

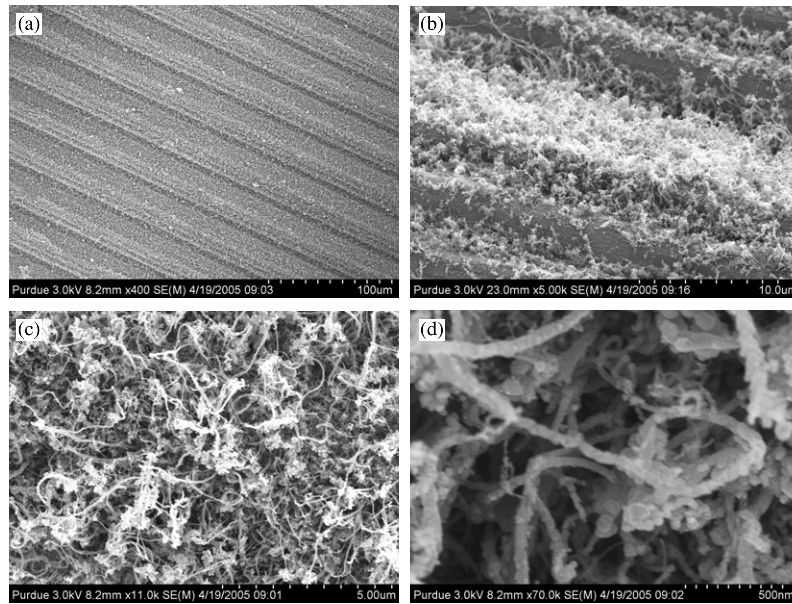


**Figure 2.** FE-SEM images of MWCNTs layer on copper substrate. (a) Machining lines on copper substrate. (b) MWCNTs on machining line. (c) Enlarged view of MWCNTs. (d) Shape of individual MWCNT.

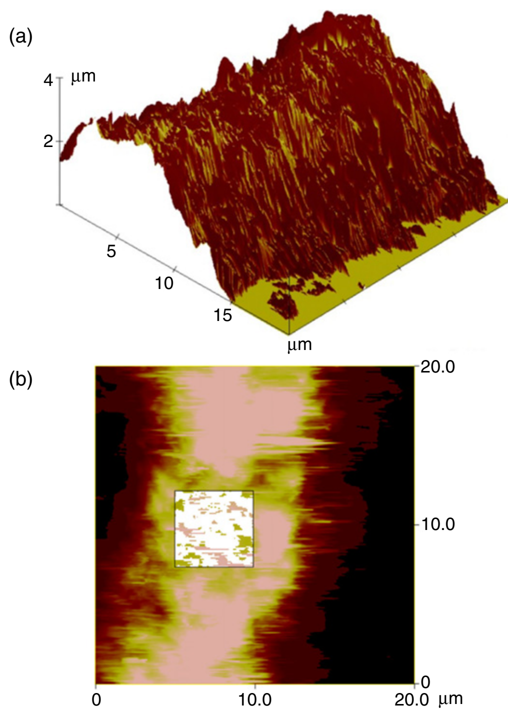


**Figure 3.** AFM images of a MWCNT layer on a machining line. (a) 3D surface height profile of MWCNT layer on the hill of machining line. (b) Surface image of MWCNT layer at the peak of a machining line.

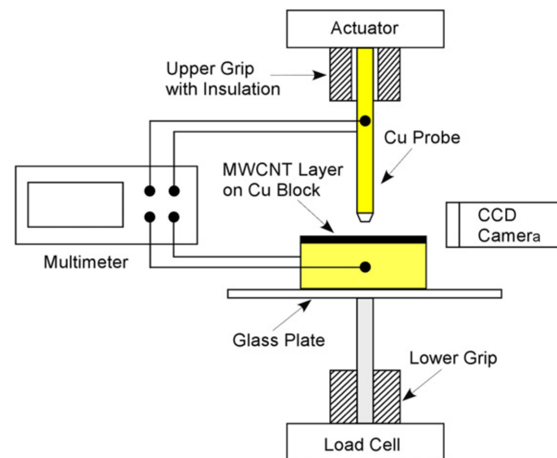


**Figure 4.** Schematic of the test setup.

was also chosen to be Cu in order to match the properties of the Cu substrate. The probe tip area is much smaller than the substrate so that multiple measurements can be made with each specimen by changing the probing location. To make the probe, the end of a copper nail was polished flat using a polisher (Buheler ECOMET V) and $Al_2O_3$ powder (size: 9–1 $\mu$m). The polished copper probe tip was observed using an optical microscope (Olympus BX60), and the image was digitized using software (Golden Software Diger 2.01) to measure the apparent surface area of the probe tip to be 0.31 mm$^2$.

A small-scale mechanical testing machine (Bose Endura ELF 3200) was used to control the probe displacement and to measure the interaction force between the probe and MWCNT-enhanced Cu substrate surface. The position of the probe tip was adjusted towards the sample surface while monitoring the position of the probe tip through a CCD camera. Starting from this non-contacting position (infinite electrical resistance), the probe was slowly displaced downwards in 1.0 $\mu$m increments until the first measurable electrical resistance was observed. This location was set to be the initial position ($Z = 0$ $\mu$m) of the probe, and the probe tip was subsequently moved downwards by 1.0 $\mu$m increments. At each displacement step,

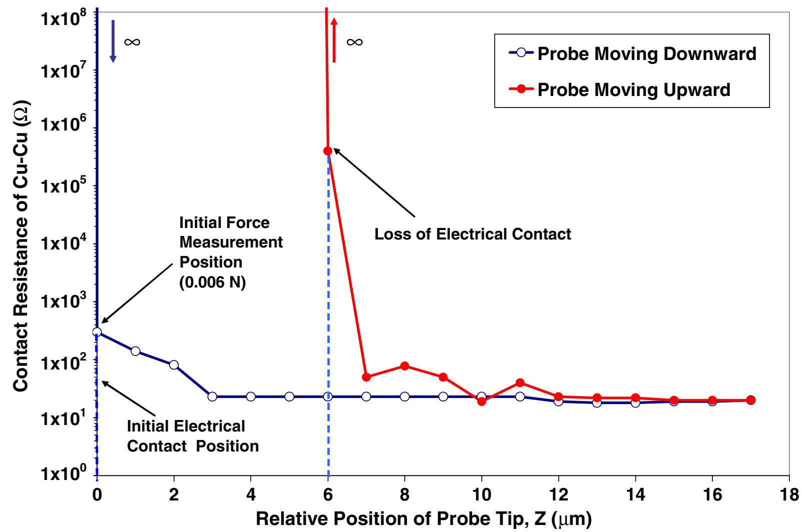


**Figure 5.** Contact resistance of a bare Cu–Cu interface as a function of probe tip position.

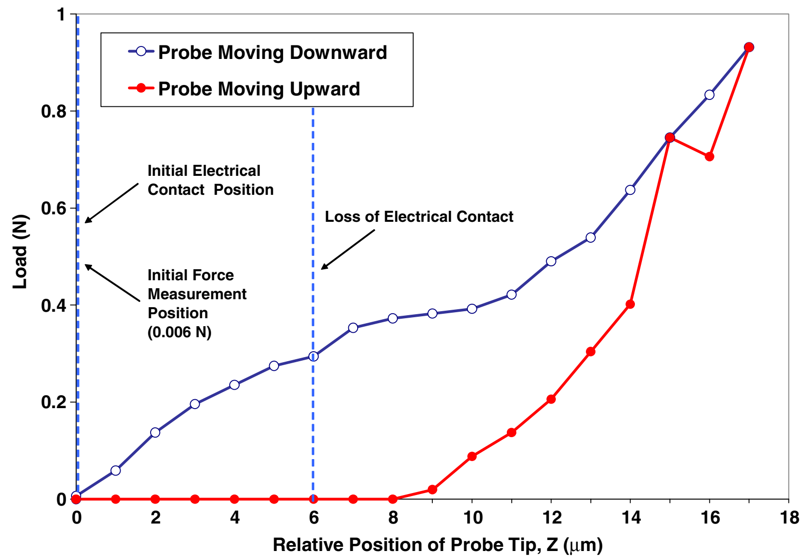


**Figure 6.** Contact force of a bare Cu–Cu interface as a function of probe tip position.

contact resistance and force data were recorded. When the resistance displayed a trend close to a constant value, the probe descent was stopped. The probe was then moved upwards (reverse direction) in 1.0 $\mu$m increments while measuring the contact resistance and force until electrical contact was lost (infinite resistance).

## 3. Experimental results

### *3.1. Bare Cu–Cu contact*

Figure 5 shows the measured electrical resistance for the Cu probe contacting a bare Cu surface, plotted as a function of probe tip displacement. These bare Cu–Cu contact data serve as a control condition. The first finite contact resistance measured was 300 $\Omega$ corresponding to an initial contact force of 0.006 N. This probe position was regarded as the initial position ($Z = 0$ $\mu$m). Note that the probe position at which initial contact resistance and force data were first obtained coincided at the same probe position. With the probe moving downwards, resistance decreased and force increased (figure 6). However, after the Cu probe passed $Z = 3$ $\mu$m, the resistance remained constant at a value of 20 $\Omega$ regardless of contact force.

The downward movement of the Cu probe was stopped at $Z = 17$ $\mu$m, and the probe was then moved upwards at 1 $\mu$m increments with resistance and force data collected as before. The resistance did not change significantly until the probe moved upwards to $Z = 7$ $\mu$m. At $Z = 6$ $\mu$m, the resistance increased to 0.4 M$\Omega$ and thereafter indicated infinite resistance. Note that electrical contact was lost before the probe reached the initial position ($Z = 0$ $\mu$m).

The contact force did not follow the same path during loading (probe moving downwards) and unloading (probe

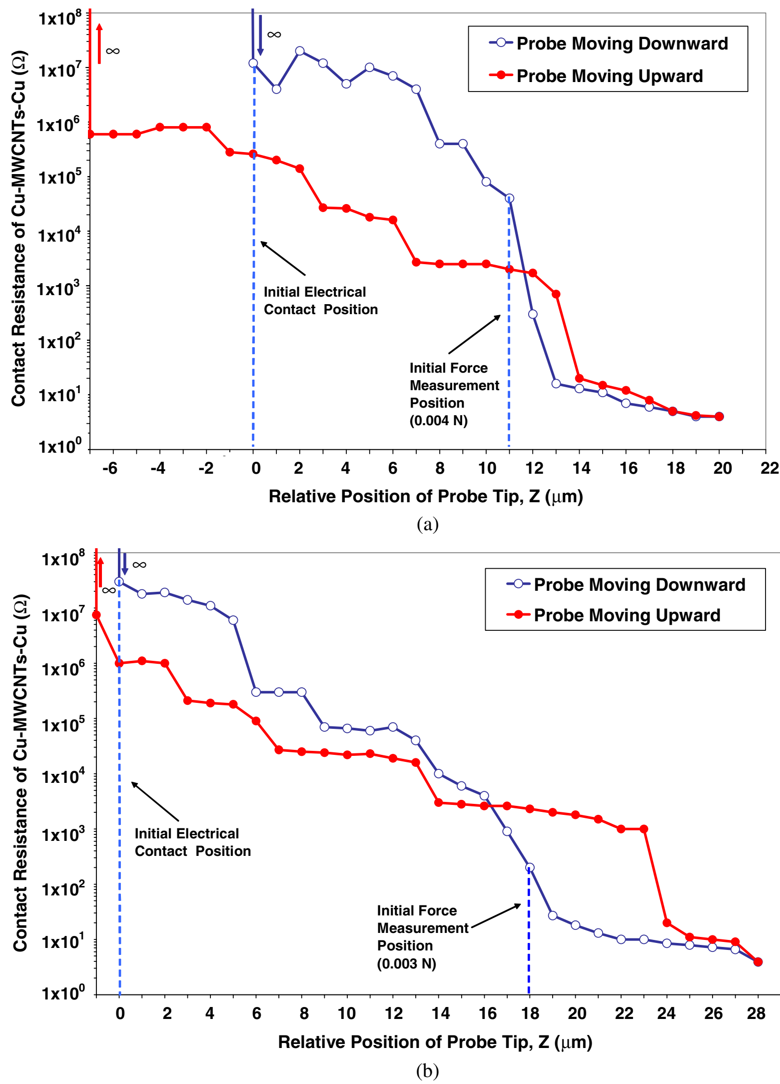


**Figure 7.** Contact resistance of a Cu–MWCNT–Cu interface as a function of probe tip. (a) Test 1; (b) Test 2.

moving upwards). This is indicated in the force–displacement measurements shown in figure 6. The contact force initially shows a linear tendency (initial stiffness: $0.067 \times 10^6$ N m$^{-1}$) and then non-linear behaviour as the probe moved downwards. Lower force values at corresponding $Z$ positions with non-linear behaviour were observed as the probe moved upwards.

### 3.2. MWCNT-enhanced contact

The change in contact resistance between the Cu probe and the MWCNT enhanced Cu substrate as a function of position is shown in figures 7(a) and (b). The measurements were conducted at two different locations on the same specimen surface, referred to as test 1 and test 2. The resistance ranged from a maximum value of $10^8$ Ω to a minimum value of 4 Ω. As the probe was lowered, resistance decreased.

In test 1, the position corresponding to the first finite resistance value shown in figure 7(a) is identified as initial electrical contact position ($Z = 0$ $\mu$m). The resistance did not change significantly until the probe moved downwards past $Z = 7$ $\mu$m. At $Z = 11$ $\mu$m, the first measurable reaction force was observed. The electrical resistance then reduced significantly to a steady value of 4 Ω with increased probe movement. Note that between the initial position ($Z = 0$ $\mu$m) and $Z = 11$ $\mu$m, there was no measurable force but electrical contact was maintained (finite resistance was measured). In test 2, the distance between the initial position ($Z = 0$ $\mu$m) and the first measurable force position ($Z = 18$ $\mu$m) is longer than that of test 1. This can be attributed to the resolution limits of the load cell and contact characteristics between the probe and MWCNT layer. In the beginning of contact, a relatively smaller number of MWCNT touch the probe tip and thus the force is in the range below the 0.001 N resolution of the load cell.

Resistance measured while the probe moved upwards (reverse process) for the first several steps (from $Z = 20$ $\mu$m to $Z = 14$ $\mu$m for test 1 and from $Z = 28$ to 24 $\mu$m for test 2) showed similar or slightly higher values at corresponding positions of the downward measurement. However, the resistance did not increase to an infinite value when the probe

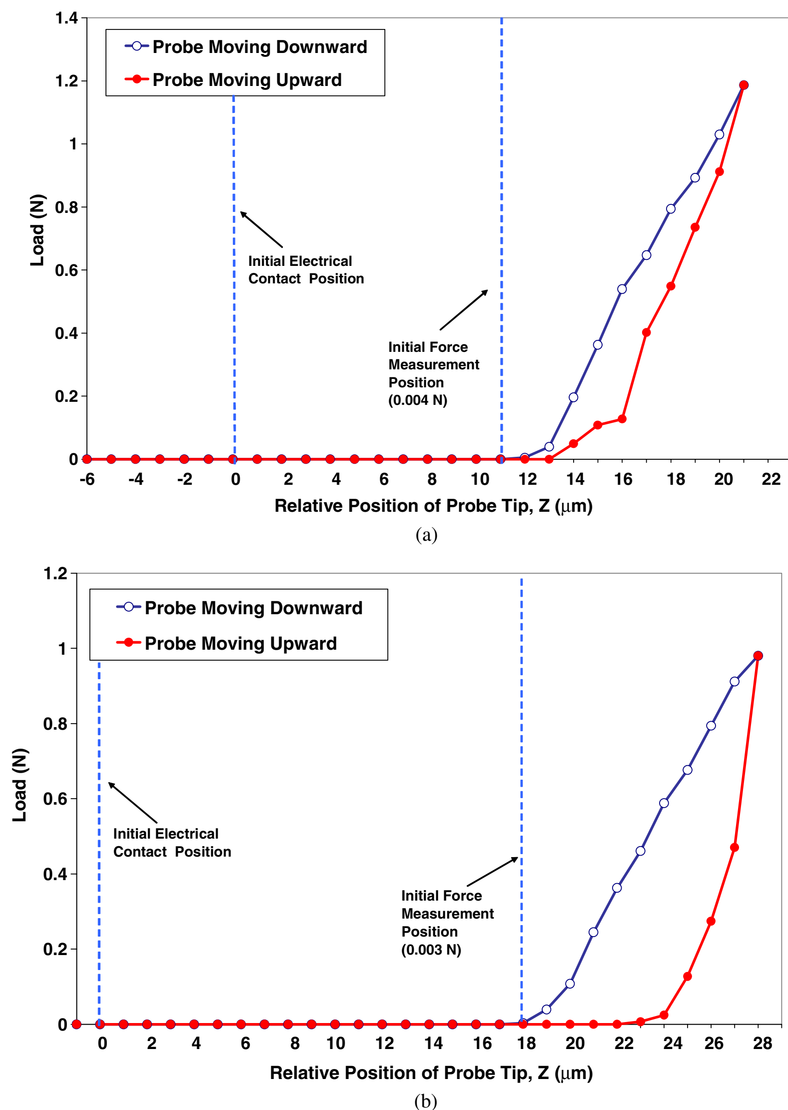


**Figure 8.** Contact force of a Cu–MWCNT–Cu interface as a function of probe tip position. (a) Test 1; (b) Test 2.

passed the position from where contact force between two surfaces dropped to zero ($Z = 13$ $\mu$m for test 1 and $Z = 23$ $\mu$m for test 2). Electrical contact is maintained even past the initial position ($Z = 0$ $\mu$m), up to $Z = -7$ $\mu$m for test 1 and to $Z = -1$ $\mu$m for test 2. This trend is opposite to that observed for the bare Cu–Cu contact. Also, step-like features of resistance change are evident during both downward and upward movements of the probe. These features are thought to be the result of van der Waals forces, which are discussed in detail later.

In figure 8, contact force is plotted as a function of probe tip displacement. The overall trend of force change is more linear than the control case (bare Cu–Cu contact plotted in figure 6). The average stiffness during downward movement ($0.173 \times 10^6$ N m$^{-1}$ for test 1 and $0.123 \times 10^6$ N m$^{-1}$ for test 2) is approximately two times higher than the initial stiffness of the bare Cu–Cu contact ($0.067 \times 10^6$ N m$^{-1}$).

The differences in the measured resistance and force between test 1 and test 2 are attributed to the global-scale variations of the MWCNT layer. The density and morphology of the MWCNT layer generally varies at different probing locations. Also, the sensitivity of the electrical resistance measurements affects how one defines the initial electrical contact position indicated in figures 7 and 8. However, it is notable that after the probe registers a measurable force, the trends of contact resistance versus force for both tests are found to closely overlap each other, as shown in figure 9.

## 4. Discussion

### *4.1. Enlargement of real contact area*

From the previous results, it is clear that the MWCNT layer played a key role in reducing electrical resistance and increasing stiffness. A comparison of the bare Cu–Cu contact and the Cu–MWCNT–Cu contact is shown in figure 9. For the same apparent contact area, the Cu–MWCNT–Cu interface showed a minimum resistance of 4 Ω, whereas the Cu–Cu interface showed a minimum resistance of 20 Ω. An 80% reduction in resistance was observed under small compressive

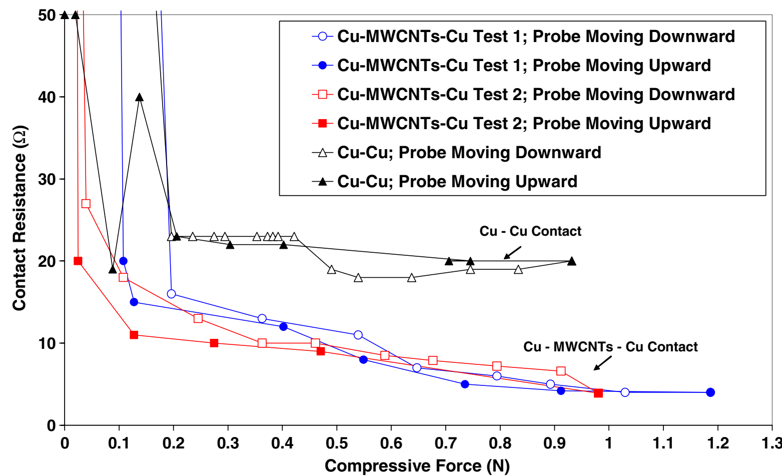


**Figure 9.** Comparison of contact resistance between a bare Cu–Cu interface and a Cu–MWCNT–Cu interface.

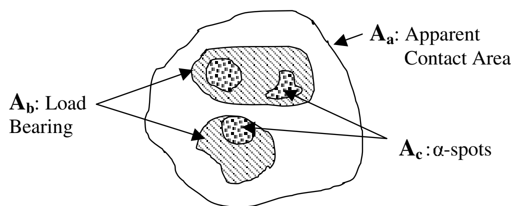


**Figure 10.** Classification of the contact surface.

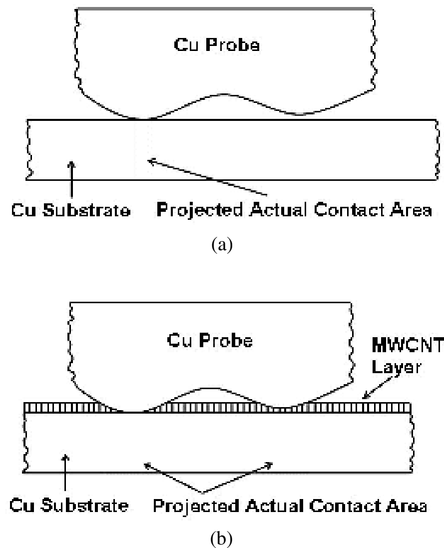


**Figure 11.** Contact resistance reduction by parallel contacts created by MWCNTs. (a) Typical contact configuration of a bare Cu–Cu contact. (b) Parallel contacts by many MWCNTs.

loading when MWCNTs were used as an interfacial material between Cu surfaces. The average stiffness of the Cu–MWCNT–Cu contact was approximately two times larger than that of the bare Cu–Cu contact.

*4.1.1. Resistance reduction mechanism.* The mechanism of contact resistance reduction due to the presence of the MWCNT layer can be explained by two phenomena: (i) enlargement of real contact area through numerous parallel contacts, (ii) electrical junctions between CNTs combined with compressive loading. Although CNTs can carry large current densities, it is known that by simply placing a single CNT on a metal electrode, the contact resistance was observed to be in the $10^3$–$10^6$ Ω range [21, 22]. Also the minimum resistance between a single CNT and a metal contact can be of the order of $10^3$ Ω [10]. However, macroscopic contact resistance can be reduced by using a MWCNT layer containing numerous individual MWCNTs that create parallel paths. Note that only a portion of the apparent contact surface, which is indicated as $A_c$ (α-spots) in figure 10, participates in electrical conduction. In the case of the Cu–MWCNT–Cu contact, CNTs significantly increase the size of $A_c$ (α-spots). Although this contact situation is very complicated, it can be simplified conceptually. As depicted in figure 11, the gap between two contacting members (see figure 11(a)) is filled with MWCNTs, thereby increasing the contact area (see figure 11(b)) via numerous parallel electrical contact paths.

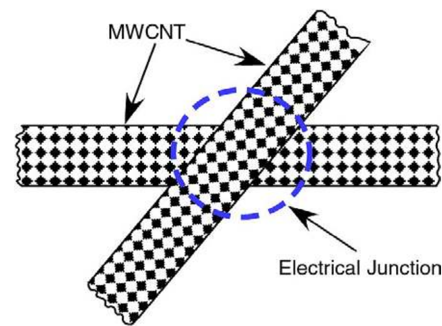


**Figure 12.** The electrical junction of two MWCNT contact surfaces.

Resistance reduction is also possible though electrical junctions made between CNTs. The MWCNTs on the substrate's surface exhibit a random configuration with no preferential direction (see figure 2). These create electrical junctions among adjacent CNTs to reduce the contact resistance as depicted in figure 12. Other researchers suggest

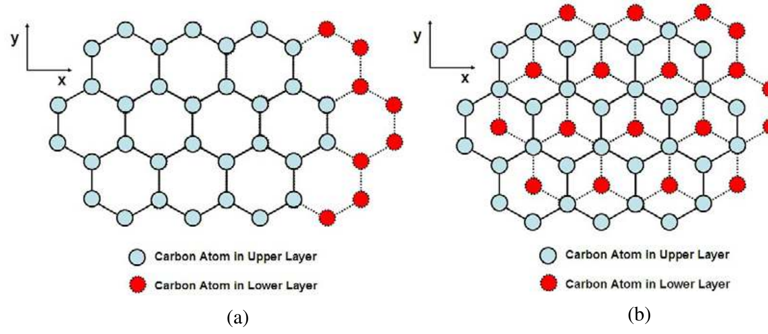


**Figure 13.** The stacking sequence of MWCNT contact surfaces. (a) A–A sequence: in registry (lower junction resistance). (b) A–B sequence: out of registry (higher junction resistance).

that contact resistances vary widely depending on the relative orientation of two CNT surfaces (see figure 13) and the level of compressive loading on the junction [23, 24]. When two contacting CNTs are in the A–A configuration, it is called 'in registry' which exhibits lower contact resistance than the A–B configuration ('out of registry'). For example, in the case of an 'in registry' junction, the resistance is 2.05 MΩ for rigid tubes [24]. If compressive force is applied on this junction, the resistance is reduced to 121 kΩ [24]. In real cases, the junction resistance probably falls between the lower and the higher resistances. Therefore, it is believed that the ensemble of the numerous contacts and junctions created during the probe movement dictate the macroscopic contact resistance.

*4.1.2. Stiffness increase.* For the Cu–MWCNT–Cu interface, the force increased almost linearly when the Cu probe moved downwards (figure 8). However for the bare Cu–Cu contact, the force did not increase in a steady manner, and was less than that of the Cu–MWCNT–Cu contact (figure 7). Note that if the load bearing area is increased, then the force will increase accordingly. Thus it can be concluded that the MWCNT layer is also effective in enlarging the load bearing area.

### 4.2. Compaction-based resistance change model

A model is presented to predict the change in contact resistance as a function of applied compressive force, as plotted in figure 9. This model is based on resistance reduction due to the compaction of the MWCNT layer beneath a probe tip of area $A$ (0.31 mm$^2$). The volume of MWCNTs beneath the probe has initial volume fraction $v_0$. During the probe's downward stroke, volume fraction $v$ is assumed to be related to strain as

$$\frac{v}{v_0} = (1 + \varepsilon) \tag{1}$$

where $\varepsilon$ is true strain, defined as positive in compression. Compressive force $F$ is observed to be linearly related to downward probe movement (see figure 8) over a roughly 8–9 $\mu$m stroke. This linear behaviour can be represented as

$$F = E_{\text{eff}} A \varepsilon \tag{2}$$

$E_{\text{eff}}$ is the effective elastic modulus of the MWCNT layer which can be found by the relationship

$$E_{\text{eff}} = \frac{L}{A} k \tag{3}$$

where $k$ is the experimentally measured stiffness in figure 8 during downward probe movement and $L$ is chosen as 8 $\mu$m. Based on equation (3), $E_{\text{eff}}$ is found to range from 3.2 to 4.5 MPa. A relationship between electrical conductance $C$ and volume fraction is now assumed to be in the form of a power law of order $n$, such that as the volume fraction of the MWCNT increases, the conductivity also increases beyond the starting value $C_0$ corresponding to the initial volume fraction $v_0$.

$$C = C_0 \left(\frac{v}{v_0}\right)^n . \tag{4}$$

Resistance is the inverse of $C$ and can be expressed as

$$R = R_0 \left(\frac{v}{v_0}\right)^{-n} . \tag{5}$$

Finally, equations (1)–(3) can be combined into equation (5), resulting in a relationship between contact resistance $R$ and probe compressive force.

$$R = R_0 \left(1 + \frac{F}{E_{\text{eff}} A}\right)^{-n} . \tag{6}$$

Parameters $R_0$ and $n$ in equation (6) are fitting constants that must be chosen to best match the resistance versus force data in figure 9. As shown in figure 14, choices of $R_0 = 26.1$ Ω and $n = 2.87$ are found to give a best fit to the pooled data (tests 1 and 2 downward stroke).

### 4.3. van der Waals interaction

Each carbon atom in a CNT is bonded to three coplanar neighbour carbon atoms by covalent bonds ($x$ and $y$ direction), and the fourth electron of each carbon atom ($z$ direction) participates in weak van der Waals bonding. Due to this molecular structure, interactions among CNTs are dominated by van der Waals forces that tend to bundle individual CNTs [25, 26]. It is hypothesized that the electrical contact measured during upward movement of the probe beyond the initial contact height is due to uprooted MWCNTs bridging the probe and substrate, thereby maintaining electrical contact (see figure 7). For the bare Cu–Cu contact, there was only local plastic deformation during downward movement, and the two Cu surfaces separated earlier during upward movement and lost electrical contact before the probe reached the initial position.

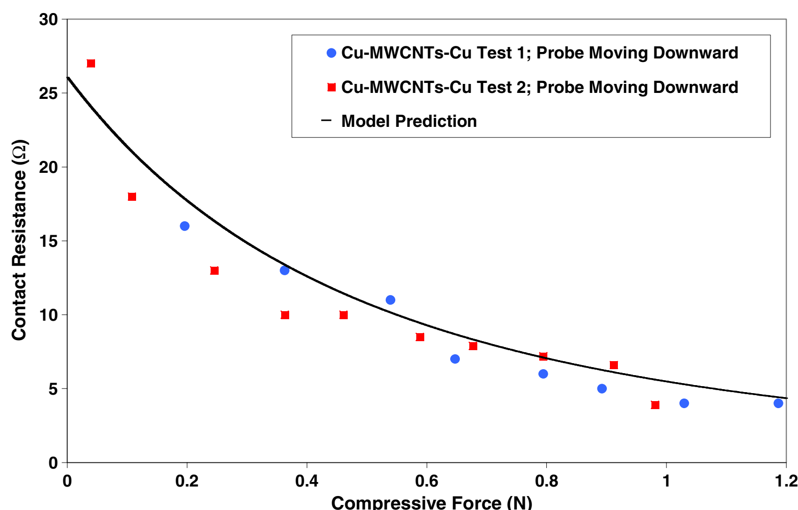


**Figure 14.** Resistance change based on compaction model.

During testing of the Cu–MWCNT–Cu contact, the resistance exhibited step-like features, especially for the higher values of resistance (see figure 7). These features were evident from data collected from the probe moving both downwards and upwards. This effect can be explained by van der Waals force interactions among MWCNTs and/or Cu surfaces as previously mentioned. It is thought that the MWCNTs formed clusters and maintained electrical contact to some extent, thereby resisting tensile forces during the probe's upward movement. When the clusters partially separate from the probe, the electrical flow path is reduced, and step-like resistance changes resulted. Note that a maximum adhesion force of 3.5 mN between MWCNTs has been reported in the literature [13]. This force is the result of a combination of the mechanical entanglement between the MWCNTs and van der Waals forces.

## 5. Conclusions

Experimental measurements have shown that a MWCNT layer between Cu–Cu surfaces reduces electrical contact resistance by 80%. This electrical resistance decrease is due to the unique structure of the MWCNT layer. Individual MWCNT are deformable, and thus when two mating surfaces come into contact, the MWCNT array creates numerous current conduction paths. Additionally, electrical junctions are formed between adjacent MWCNTs, further reducing contact resistance. MWCNT-enhanced Cu surfaces showed approximately two times higher surface stiffness, thereby indicating that both the electrical contact and load bearing area were increased due to the presence of the MWCNT layer. MWCNT-enhanced Cu surfaces exhibited step-like resistance changes and maintained electrical contact over a larger distance than bare Cu–Cu contact, particularly during movement of the contacting probe away from the surface. It is hypothesized that this is due to uprooted MWCNTs bridging the probe and substrate via van der Waals forces, thereby maintaining electrical contact during probe movement. The MWCNT-enhanced surface showed a finite slope of electrical resistance as a function of contact force, thereby making it possible to use this arrangement as a small-scale force or pressure sensor. Finally, a model based on compaction of the MWCNT layer was presented and found to be capable of predicting the change in contact resistance as a function of probe compressive force.

## Acknowledgments

This research was supported by the Purdue Research Foundation. Jun Xu and Timothy S Fisher gratefully acknowledge support from the National Science Foundation, Chemical and Transport Systems. The authors also would like to thank Xi Richard Zhang, Placidus Amama, John Philips, and Tim Miller for discussion and help at different stages of this research.

## References

[1] Holm R 1967 *Electric Contacts* (New York: Springer) pp 7–52
[2] Timsit R S 1999 Electrical contact resistance: properties of stationary interfaces *IEEE Tran. Compon. Packag. Technol.* **22** 85–98
[3] Iijima S 1991 Helical microtube of graphitic carbon *Nature* **354** 56–8
[4] Barber A H, Cohen S R and Wagner H D 2003 Measurement of carbon nanotube–polymer interfacial strength *Appl. Phys. Lett.* **82** 4140–2
[5] Ebbesen T W, Lezec H J, Hiura H, Bennett J W, Ghaemi H F and Thio T 1996 Electrical conductivity of individual carbon nanotubes *Nature* **382** 54–6
[6] Treacy M M J, Ebbesen T W and Gibson J M 1996 Exceptionally high Young's modulus observed for individual carbon nanotubes *Nature* **381** 678–80
[7] Nakanishi T, Bachtold A and Dekker C 2002 Transport through the interface between a semiconducting carbon nanotube and a metal electrode *Phys. Rev.* B **66** 073307
[8] Wang X, Liu Y, Yu G, Xu C, Zhang J and Zhu D 2001 Anisotropic electrical transport properties of aligned carbon nanotube films *J. Phys. Chem.* B **105** 9422–5
[9] Datta S 1991 *Quantum Transport: Atom to Transistor* (Cambridge: Cambridge Press)
[10] Srivastava N and Banerjee K 2004 A comparative scaling analysis of metallic and carbon nanotube interconnections

for nanometer scale VLSI technologies *Proc. 21st Int. VLSI Multilevel Int. Conf.* pp 393–8

[11] Graugnard E D 2000 The electronic properties of multi-walled carbon nanotubes *PhD Thesis* Purdue University pp 53–64

[12] Xu J and Fisher T S 2004 Thermal contact conductance enhancement with carbon nanotube array *Proc. IMECE 2004, ASME Int. Mechanical Engineering Congress and RD&D Expo.* pp 1–5

[13] Tong T, Zhao Y, Delzeit L, Majumdar A and Kashani A 2004 Multiwalled carbon nanotube/nanofiber arrays as conductive and dry adhesive interface materials *Proc. Nano 2004, ASME Integrated Nanosystems* pp 1–6

[14] Smith W F *Structure and Properties of Engineering Alloys* 2nd edn (New York: McGraw-Hill) pp 233–43

[15] You L, Chang W T and Tabib-Azar M 2004 Selective growth of carbon nanotubes by catalyst poisoning *Annual APS March Meeting 2004 (Montreal, Quebec, Canada)*

[16] Cassell A M, Franklin N R, Tombler T W, Chan E M, Han J and Dai H 1999 Directed growth of free-standing single-walled carbon nanotubes *J. Am. Chem. Soc.* **121** 7975–6

[17] Kato T, Jeong G H, Hirata T and Hatakeyama R 2004 Structure control of carbon nanotubes using radio-frequency plasma enhanced chemical vapour deposition *Thin Solid Films* **457** 2–6

[18] Ho G W, Wee A T S, Lin J and Tjiu W C 2001 Synthesis of well-aligned multiwalled carbon nanotubes on Ni catalyst using radio frequency plasma-enhanced chemical vapour deposition *Thin Solid Films* **388** 73–7

[19] Howland R and Benatar L 2000 *A Practical Guide to Scanning Probe Microscopy* Park Scientific instruments, p 8 http://web.mit.edu/cortiz/www/AFMGallery/PracticalGuide.pdf

[20] Pfeiffer G, Fetheroff S and Iyer S S 1995 Final polish for SOI wafers—surface roughness and TTV degradation *Proc. 1995 IEEE Int. SOI Conf.* pp 172–3

[21] Tzeng Y, Chen Y and Liu C 2003 Electrical contacts between carbon-nanotube coated electrode *Diamond Relat. Mater.* **12** 774–9

[22] Wei B Q, Vajtai R and Ajayan P M 2001 Relability and current carrying capacity of carbon nanotubes *Appl. Phys. Lett.* **79** 1172–4

[23] Fuhrer M S *et al* 2000 Crossed nanotube junctions *Science* **288** 494–7

[24] Buldum A and Lu J P 2001 Contact resistance between carbon nanotubes *Phys. Rev.* B **63** 161403(R)

[25] Song S N, Wang X K, Chang R P H and Ketterson J B 1994 Electronic properties of graphitic nanotubles from galvanomagnetic effects *Phys. Rev. Lett.* **72** 697–700

[26] Callister W D Jr 1997 *Materials Science and Engineering—An Introduction* 4th edn, pp 389–90